ICASSP 2024 - 2024 IEEE International Conference on Acoustics, Speech and Signal Processing (ICASSP) | 979-8-3503-4485-1/24/$31.00 ©2024 IEEE | DOI: 10.1109/ICASSP48485.2024.10447858

DETECTOR DESIGN FOR DISTRIBUTED MULTICHANNEL RADAR SENSORS IN COLORED INTERFERENCE ENVIRONMENTS

Moein Ahmadi, Mohammad Alaee-Kerahroodi, Linlong Wu, Bhavani Shankar M. R., and Björn Ottersten

Interdisciplinary Centre for Security, Reliability and Trust (SnT), University of Luxembourg

ABSTRACT

In this paper, we present a generic signal model applicable to various distributed radar setups, encompassing both phased array (PA) and MIMO radar configurations. We consider a range of waveform modulation methods, including TDM, BPM, DDM, and fast time CDM. We devise a GLRT based detector for scenarios where the interference consists of colored noise plus a signal in a low-rank subspace and prove that the designed detector is CFAR. We demonstrate that when the CPI time is similar for the systems, the PA radar system exhibits better detection performance than MIMO, irrespective of the waveform modulation approach adopted. However, if the CPI time of the PA system is divided to the number of transmit waveforms utilized in the MIMO radar case (to account for the time needed for a PA radar to scan all angles), then in the presence of non-uniform interference, MIMO techniques, except TDM, surpass the performance of PA. Conversely, in cases of uniform interference, the performance of both MIMO techniques and PA are equivalent.

***Index Terms*—** Adaptive detection, clutter subspace, distributed MIMO radar, GLRT, indoor sensing.

1. INTRODUCTION

Multichannel radar equipped with multiple transmit/receive (TX/RX) antennas, has been of considerable interest for automotive and indoor monitoring applications in recent years [1–3]. The conventional assumption on colocated Multiple-Input Multiple-Output (MIMO) radar is that, the spatial resolution can be improved by increasing the number of antenna elements in the Virtual Array (VA), which is ensured by the orthogonality among transmitted waveforms [4]. In this context, the waveform orthogonality can be obtained in one pulse using Frequency Division Multiplexing (FDM) [5] or fast time Code Division Multiplexing (CDM) [6] technique or in multiple pulses using Time Division Multiplexing (TDM), Binary Phase Modulation (BPM), Doppler Division Multiplexing (DDM) techniques [7], [8], [9]. In this paper, we propose a general signal model for multichannel radars, which includes all the aforementioned multiplexing schemes. The signal model for a Phased Array (PA) is considered as a special case of the proposed general signal model. In line with [10], this paper shows that contrary to claims made, colocated MIMO radars do not provide an order of magnitude or better angle resolution than thin-full PA radars. A large number of works have been devoted to the development of distributed MIMO radar detection in homogeneous [11] and non-homogeneous [12, 13] clutter environments, low-complexity multi-target detection and localization [14] and considering non-orthogonal waveforms [15]. In our previous study [16], we illustrated that in a scenario when multiple MIMO radar sensors are connected, a detector can be designed for the case when exact information about the interference subspace is available. In contrast to our earlier study, in this paper, we consider the problem of detector design for distributed MIMO radar systems, when the interference subspace can be divided into two components: one with readily available subspace information and the other containing interference with unknown subspace structure. In such instances, the unidentified part of the interfering signal can be treated as colored noise. Based on the signal model, we derive a Generalized Likelihood Ratio Test (GLRT) detector and its statistical properties in closed form for both the null and alternative hypotheses. Furthermore, we demonstrate analytically that the proposed GLRT is a CFAR detector. We show that the proposed detector outperforms Adaptive Matched Filter (AMF) [16, 17] and the subspace detector [16, 18] when the interference to noise ratio is high. Also, besides analyzing the detector statistically, we assess the detection performance of various multiplexing techniques, including TDM, DDM, BPM, CDM, and PA, in relation to the derived generic signal model. PA radar focuses its beam in a single transmit direction in a coherent pulse interval and therefore it needs more time to scan the entire environment. This paper demonstrates that when the same CPI time is used for both PA and MIMO radar systems, regardless of the waveform modulation scheme employed in the MIMO system, the detection performance of PA is superior to that of the MIMO radar system. We show that if the CPI time for PA be divided by the number of transmit waveforms in the MIMO radar system, then in homogeneous environment, all the multiplexing techniques excluding TDM exhibit identical detection performance to that of PA. Nonetheless, in nonhomogeneous environment, MIMO techniques (except TDM) surpass the performance of PA.

This work was supported by FNR BRIDGES MASTERS under grant BRIDGES2020/IS/15407066/MASTERS.

2. SIGNAL MODEL

We consider a distributed radar system with Q colocated multichannel radar sensors, each have M_q transmit antenna elements, and N_q receive antenna elements. Assume that the qth radar sensor is located at absolute Cartesian position $\mathbf{p}_q$ and there are some targets which each target represented by parameters $\Theta = [\mathbf{p}_s, \mathbf{v}_s, \alpha, c_{id}]$ where $\mathbf{p}_s$ and $\mathbf{v}_s$ are absolute position and velocity vector of the target, respectively. $\alpha = [\alpha_1, \cdots, \alpha_Q]$ is the target amplitude in the sensors and c_{id} is the target microDoppler class which is used in target identification applications. The target will have a relative distance R_q, azimuth θ_q, and elevation ϕ_q with the qth radar sensor. Without loss of generality, for the sensor q, one range cell R_q, which contains I_q targets with different angles and different velocities, is assumed. After range focus processing (i.e. range FFT (stretch processing) in FMCW radars or range matched filtering for other conventional radars), the received signal from L_q pulses in one Coherent Processing Interval (CPI) can be expressed as, $\mathbf{x}_q = \sum_{i=1}^{I_q} \alpha_{q,i}\mathbf{s}_q(\theta_{q,i}, \phi_{q,i}, f_{d,q,i}) + \mathbf{n}_q$ where $\alpha_{q,i}$ indicates the amplitude of the reflected signal for ith scatter at the qth radar sensors and $\mathbf{n}_q$ is the interference signal for this sensor. The signal steering vector is $\mathbf{s}_q(\theta, \phi, f_d) = \mathbf{u}_q(\theta, \phi, f_d) \otimes \mathbf{b}_q(\theta, \phi)$ where $\mathbf{b}_q(\theta, \phi)$ is the received steering vector as defined in [16] and $\mathbf{u}_q(\theta, \phi, f_d)$ is the transmit-Doppler steering vector that we define it for two category of waveform multiplexing techniques. For CDM radars (we call it herein *single pulse waveform multiplexing technique*),

$$\mathbf{u}_q^S(\theta, \phi, f_d) = \mathbf{a}_q(\theta, \phi) \otimes \mathbf{d}_q(f_d) \in \mathbb{C}^{M_q L_q} \tag{1}$$

and for TDM, BPM, and DDM-MIMO techniques (we call it herein *multiple pulse waveform multiplexing techniques*) and also for the PA radars,

$$\mathbf{u}_q^M(\theta, \phi, f_d) = (\mathbf{W}_q \mathbf{a}_q(\theta, \phi)) \odot \mathbf{d}_q(f_d) \in \mathbb{C}^{L_q} \tag{2}$$

where $\mathbf{a}_q(\theta, \phi)$ and $\mathbf{d}_q(f_d)$ are transmit and Doppler steering vectors, respectively [16]. $\mathbf{W}_q$ is the slow time precoding matrix and is defined for multiple pulse waveform multiplexing techniques and PA radars.

In TDM MIMO radar, the transmitters are successively transmitted following the fixed periodic order, then $\mathbf{W}_q^{TDM} = [\underbrace{\mathbf{I}_{M_q}, \mathbf{I}_{M_q}, \cdots, \mathbf{I}_{M_q}}_{K|L_q=KM_q}]^T$ where $K = L_q/M_q$ should be an integer. Although TDM offers ease of implementation, it is associated with a drawback: it experiences a decline in transmission energy and therefore Signal to Clutter plus Interference and Noise Ratio (SCINR) and detection performance. DDM technique, as an alternative transmission method, involves phase modulation for each transmitting component from one pulse to the next. With the DDM method, the full potential of the transmitting array can be leveraged since all transmission components operate simultaneously at all moments. However, this waveform diversity comes with the trade-off of a maximum unambiguous velocity or doppler resolution depend on the precoding matrix. For maximum doppler resolution requirement, which leads to mimimum unambiguous velocity, precoding matrix elements can be defined as $\mathbf{W}_{q,l,m}^{DDM} = e^{-j2\pi ml/M_q}$. To have maximum unambiguous velocity, which leads to mimimum doppler resolution, elements of $\mathbf{W}$ can be defined as $\mathbf{W}_{q,l,m}^{DDM_2} = e^{-j2\pi ml/L_q}$ Several techniques exist to enhance the unambiguous velocity in DDM MIMO radars [9], which can be used to define precoding matrix for the proposed signal model. Further, BPM is another multiplexing scheme which utilizes Hadamard coding to indicate perfect orthogonality in slow-time. However, the number of transmission elements and the code's length are limited by the intrinsic properties of the Hadamard matrix, that means M_q, $M_q/12$ or $M_q/20$ must be a power of 2. For the BPM technique $\mathbf{W}$ is $\mathbf{W}_q^{BPM} = [\underbrace{\mathbf{H}_{M_q}, \mathbf{H}_{M_q}, \cdots, \mathbf{H}_{M_q}}_{K|L_q=KM_q}]^T$ The precoding matrix for PA radar at the specific focusing angles θ_0, ϕ_0 can be expressed by $\mathbf{W}_{q,l,m}^{PA,(\theta_0,\phi_0)} = e^{j\mathbf{k}^T(\theta_0,\phi_0)\mathbf{p}_{q,m}^{tx}}$ where $\mathbf{k}$ is the wavenumber vector, and $\mathbf{p}_{q,i}^{tx}$ is the relative position of the ith transmit element to phase center of the qth sensor [16]. Note that the PA precoding matrix elements are independent from pulse index. In Figure 1, Doppler angle beampattern for the proposed techniques are shown. It can be seen that for same antenna configurations, all multichannel techniques have **same angle resolution** and contrary to claims made, colocated MIMO radars do not provide an order of magnitude or better angle resolution than thin-full PA radars. Different angle Doppler beampatterns can be used to design the radar system for Doppler resolution and unambiguous velocity requirements. To this end, the signal model for a colocated multichannel radar is presented. For distributed radars, at the fusion center, the received signals can be stacked and $\mathbf{x} = [\mathbf{x}_1^T, \mathbf{x}_2^T, ..., \mathbf{x}_Q^T]^T$. In [16], the following detection problem is defined as $\mathcal{H}_0 : \mathbf{x} = \mathbf{Ag} + \mathbf{n}$ and $\mathcal{H}_1 : \mathbf{x} = \mathbf{S}\boldsymbol{\alpha} + \mathbf{Ag} + \mathbf{n}$ where $\mathcal{H}_0$ represent the null hypothesis that the target is absent, and $\mathcal{H}_1$ represent the alternative hypothesis that the target is present. Our previous work considers the white Gaussian noise for $\mathbf{n}$, and in this work it is generalized to colored noise $\mathbf{n} \sim \mathcal{CN}(\mathbf{0}, \mathbf{M})$, where $\mathbf{M} = \widetilde{\mathbf{M}} + \sigma_n^2\mathbf{I}$, with $\widetilde{\mathbf{M}}$ is the covariance matrix of the statistical part of interference, σ_n^2 is the variance of white Gaussian noise, and $\mathbf{A}$ is the subspace matrix of clutter and $\mathbf{g}$ is an unknown deterministic complex vector coefficients.

3. GLRT-BASED DETECTOR DESIGN

The Generalized Likelihood Ratio Test (GLRT) detector is obtained by, $t_{\text{GLRT}} = \ln \frac{\max_{\mathbf{g},\boldsymbol{\alpha}} p(\mathbf{x}|\mathcal{H}_1)}{\max_{\mathbf{g}} p(\mathbf{x}|\mathcal{H}_0)} \underset{\mathcal{H}_0}{\overset{\mathcal{H}_1}{\gtrless}} \eta$, where $p(\mathbf{x}|\mathcal{H}_0)$ and $p(\mathbf{x}|\mathcal{H}_1)$ are the Probability Density Function (PDF) of $\mathbf{x}$ under $\mathcal{H}_0$ and $\mathcal{H}_1$, respectively and $p(\mathbf{x}|\mathcal{H}_0) = \frac{1}{\pi^\Omega|\mathbf{M}|} \exp(-(\mathbf{x}-$

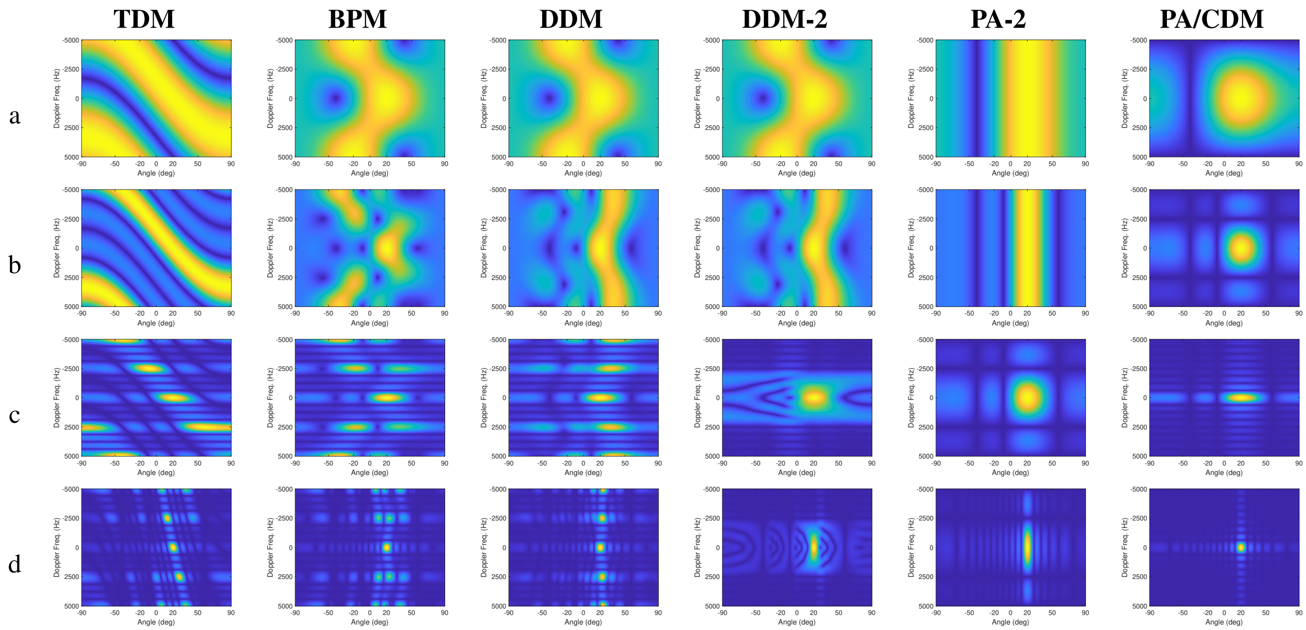

Fig. 1: Doppler angle beampattern for TDM, BPM, DDM, PA and CDM techniques ,a) $M = 2$, $N = 1$, $L = 2$, b) $M = 4$, $N = 1$, $L = 4$, c) $M = 4$, $N = 1$, $L = 16$, d) $M = 4$, $N = 4$, $L = 16$. PA-2 refers to the case when the same scan time for PA and MIMO has been considered, and consequently the CPI time for PA is divided to the number of transmit waveforms.

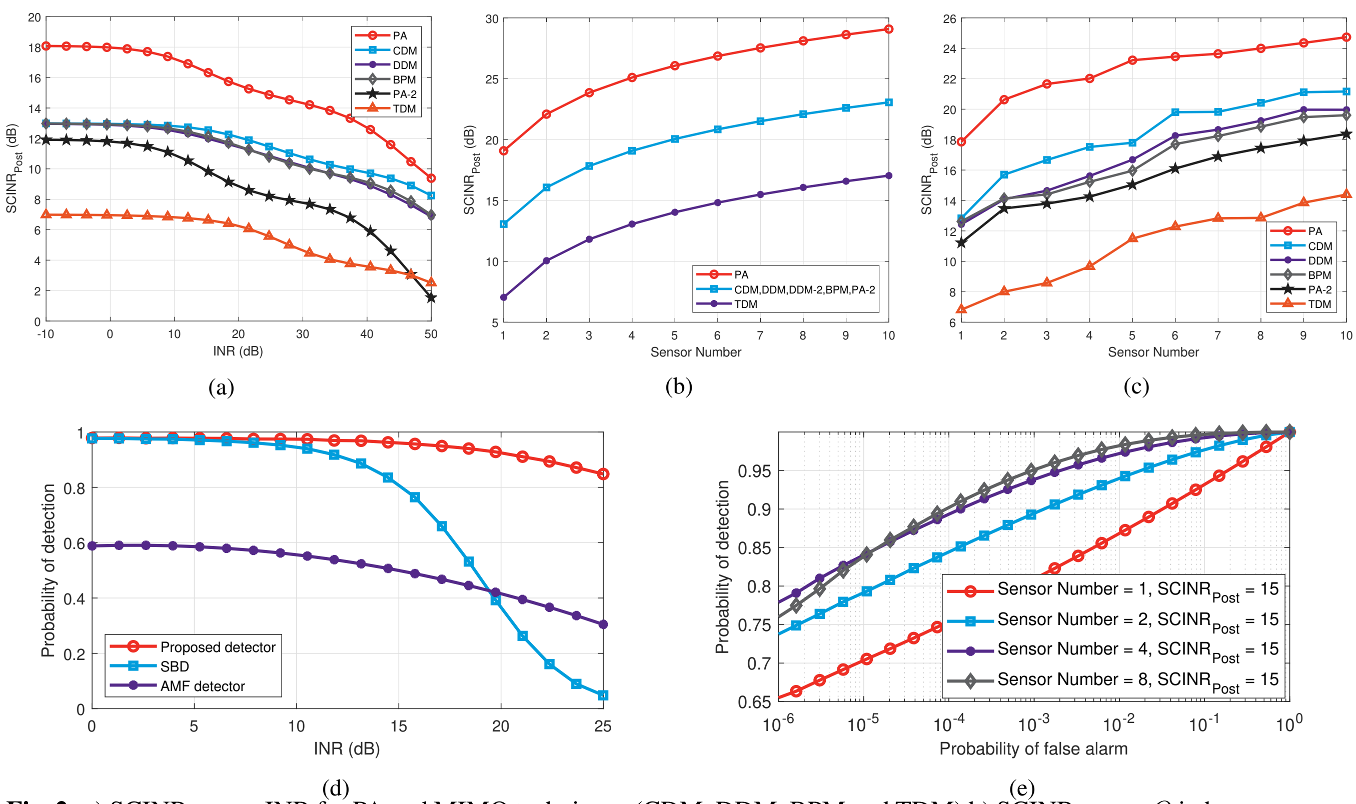

Fig. 2: a) SCINR$_{\text{Post}}$ vs. INR for PA and MIMO techniques (CDM, DDM, BPM and TDM) b) SCINR$_{\text{Post}}$ vs. Q in homogeneous env., c) SCINR$_{\text{Post}}$ vs. Q in nonhomogeneous env. d) Probability of detection vs INR for proposed detector, subspace detector [16] and AMF detector [19]. e) Receiver Operating Characteristic (ROC) for proposed detector and $Q = 1, 2, 4, 8$ distributed sensors with same SCINR$_{\text{Post}}$ and fluctuant RCS.

$\mathbf{Ag})^H\mathbf{M}^{-1}(\mathbf{x}-\mathbf{Ag}))$ and $p(\mathbf{x}|\mathcal{H}_1)=p(\mathbf{x}-\mathbf{S}\boldsymbol{\alpha}|\mathcal{H}_0)$ where $\Omega=\sum_{q=1}^{Q}L_qM_qN_q$.

Under alternative hypothesis, $\mathcal{H}_1$, the Maximum Likelihood (ML) estimations for $\mathbf{g}$ and $\boldsymbol{\alpha}$ can be obtained by solving

$$\min_{\mathbf{g},\boldsymbol{\alpha}}(\mathbf{x}-\mathbf{S}\boldsymbol{\alpha}-\mathbf{Ag})^H\mathbf{M}^{-1}(\mathbf{x}-\mathbf{S}\boldsymbol{\alpha}-\mathbf{Ag}). \tag{3}$$

The maximum likelihood estimation of the interference coefficient vector under $\mathcal{H}_1$ is given by

$$\hat{\mathbf{g}}_1=(\mathbf{A}^H\mathbf{M}^{-1}\mathbf{A})^{-1}\mathbf{A}^H\mathbf{M}^{-1}(\mathbf{x}-\mathbf{S}\boldsymbol{\alpha}) \tag{4}$$

with substituting (4) in (3), the ML estimation of $\boldsymbol{\alpha}$ is $\min_{\boldsymbol{\alpha}}(\mathbf{x}-\mathbf{S}\boldsymbol{\alpha})^H(\mathbf{I}-\mathbf{M}^{-1}\mathbf{A}(\mathbf{A}^H\mathbf{M}^{-1}\mathbf{A})^{-1}\mathbf{A}^H)\mathbf{M}^{-1}(\mathbf{I}-\mathbf{A}(\mathbf{A}^H\mathbf{M}^{-1}\mathbf{A})^{-1}\mathbf{A}^H\mathbf{M}^{-1})(\mathbf{x}-\mathbf{S}\boldsymbol{\alpha})=\min_{\boldsymbol{\alpha}}(\mathbf{x}-\mathbf{S}\boldsymbol{\alpha})^H(\mathbf{M}^{-1}-\mathbf{M}^{-1}\mathbf{A}(\mathbf{A}^H\mathbf{M}^{-1}\mathbf{A})^{-1}\mathbf{A}^H\mathbf{M}^{-1})(\mathbf{x}-\mathbf{S}\boldsymbol{\alpha})$ then the maximum likelihood estimation of $\boldsymbol{\alpha}$ under $\mathcal{H}_1$ is given by

$$\hat{\boldsymbol{\alpha}}=(\mathbf{S}^H\mathbf{P}_{\mathbf{M},\mathbf{A}}^{\perp}\mathbf{S})^{-1}\mathbf{S}^H\mathbf{P}_{\mathbf{M},\mathbf{A}}^{\perp}\mathbf{x} \tag{5}$$

where $\mathbf{P}_{\mathbf{M},\mathbf{A}}^{\perp}=\mathbf{M}^{-1}-\mathbf{M}^{-1}\mathbf{A}(\mathbf{A}^H\mathbf{M}^{-1}\mathbf{A})^{-1}\mathbf{A}^H\mathbf{M}^{-1}$. By setting $\boldsymbol{\alpha}=\mathbf{0}$ in (4), the ML estimation of $\mathbf{g}$ under $\mathcal{H}_0$ is,

$$\hat{\mathbf{g}}_0=(\mathbf{A}^H\mathbf{M}^{-1}\mathbf{A})^{-1}\mathbf{A}^H\mathbf{M}^{-1}\mathbf{x} \tag{6}$$

Substituting (4),(5) and (6) in GLRT equation lead to

$$t_{\text{GLRT}}=\mathbf{x}^H\mathbf{P}_{\mathbf{M},\mathbf{A}}^{\perp}\mathbf{S}(\mathbf{S}^H\mathbf{P}_{\mathbf{M},\mathbf{A}}^{\perp}\mathbf{S})^{-1}\mathbf{S}^H\mathbf{P}_{\mathbf{M},\mathbf{A}}^{\perp}\mathbf{x}\underset{\mathrm{H}_0}{\overset{\mathrm{H}_1}{\gtrless}}\eta \tag{7}$$

Since $\mathbf{P}_{\mathbf{M},\mathbf{A}}^{\perp}=\mathbf{M}^{-1/2}\mathbf{P}_{\mathbf{M}^{-1/2}\mathbf{A}}^{\perp}\mathbf{M}^{-1/2}$ where $\mathbf{P}_{\mathbf{B}}^{\perp}=\mathbf{I}-\mathbf{B}(\mathbf{B}^H\mathbf{B})^{-1}\mathbf{B}^H$ is the orthogonal projection on the subspace spanned by matrix $\mathbf{B}$, the test variable can be expressed as a quadratic function of $\mathbf{M}^{-1/2}\mathbf{x}$. Therefore the noise component of $\mathbf{M}^{-1/2}\mathbf{x}$ has complex Gaussian distribution with zero mean and covariance matrix $\mathbf{I}$. Due to $\mathbf{P}_{\mathbf{M},\mathbf{A}}^{\perp}\mathbf{A}=\mathbf{0}$, and also because $\mathbf{S}^H\mathbf{P}_{\mathbf{M},\mathbf{A}}^{\perp}\mathbf{S}$ is a full-rank matrix, then $\operatorname{rank}(\mathbf{P}_{\mathbf{M},\mathbf{A}}^{\perp}\mathbf{S}(\mathbf{S}^H\mathbf{P}_{\mathbf{M},\mathbf{A}}^{\perp}\mathbf{S})^{-1}\mathbf{S}^H\mathbf{P}_{\mathbf{M},\mathbf{A}}^{\perp})=Q$, and the statistical distributions of the GLRT test variable (7) under the null and alternative hypothese is the same as [16], $t_{\text{GLRT},\mathcal{H}_0}\sim\chi_{2Q}^2(0)$. Consequently, the probability of false alarm of GLRT detector is given by $P_{fa}=\Pr(t_{\text{GLRT}}>\eta|\mathcal{H}_0)=e^{-\eta}\sum_{q=0}^{Q-1}\frac{\eta^q}{q!}$. Note that the probability of false alarm is independent of the nuisance parameters, i.e., $\mathbf{g}$ and the noise variance $\mathbf{M}$, and hence, the proposed detector is a constant false alarm rate detector.

The test variable under alternative hypothesis, $t_{\text{GLRT},\mathcal{H}_1}\sim\chi_{2Q}^2(\boldsymbol{\alpha}^H\mathbf{S}^H\mathbf{P}_{\mathbf{M},\mathbf{A}}^{\perp}\mathbf{S}\boldsymbol{\alpha})$ has a noncentral chi-square distribution with $2Q$ degrees of freedom and noncentrality parameter $\boldsymbol{\alpha}^H\mathbf{S}^H\mathbf{P}_{\mathbf{M},\mathbf{A}}^{\perp}\mathbf{S}\boldsymbol{\alpha}$. The probability of detection of GLRT detector is given by $P_d=\Pr(t_{\text{GLRT}}>\eta|\mathcal{H}_1)=\mathcal{M}_Q\left(\sqrt{2\boldsymbol{\alpha}^H\mathbf{S}^H\mathbf{P}_{\mathbf{M},\mathbf{A}}^{\perp}\mathbf{S}\boldsymbol{\alpha}},\sqrt{2\eta}\right)$, where $\mathcal{M}_K(a,b)$, is the Marcum Q-function and $I_k(.)$ is the modified Bessel function of the first kind of order k. Defining Clutter to Noise Ratio (CNR) $=\frac{\mathbf{g}^H\mathbf{A}^H\mathbf{Ag}}{\Omega\sigma_n^2}$, and Interference to Noise Ratio (INR)= $\frac{\text{trace}(\widetilde{\mathbf{M}})}{\Omega\sigma_n^2}$ and the post processing signal to clutter, interference pulse noise ratio as $\text{SCINR}_{\text{Post}}=\boldsymbol{\alpha}^H\mathbf{S}^H\mathbf{P}_{\mathbf{M},\mathbf{A}}^{\perp}\mathbf{S}\boldsymbol{\alpha}$ results in $P_d=\mathcal{M}_Q(\sqrt{2\text{SCINR}_{\text{Post}}},\sqrt{2\eta})$. The calculated probability of false alarm and probability of detection closely resembles the findings in [16], where white noise is taken into account. The sole distinction lies in the $\text{SCINR}_{\text{Post}}$. Given the analysis and results from [16], complementary simulations will be presented in the subsequent section.

4. SIMULATION AND RESULTS

In this section, simulation examples are performed to demonstrate the performance of proposed detector. For all simulations, colocated multichannel radar equipped with 4 receive antennas with half-wavelength distance and 4 transmit antenna with 2 wavelength distance. In Figure 2, SCINR performance for different techniques is shown. In these figures, when the number of pulses in each CPI is unique for all the systems, PA exhibits better performance than MIMO. However, if the CPI time of the PA be divided to the number of transmit waveforms utilized in the MIMO radar case (PA-2), then in the presence of non-uniform interference (Figure 2c), MIMO techniques, except TDM, surpass the performance of PA. Conversely, in case of uniform interference, the performance of both MIMO techniques and PA are equivalent (Figure 2a, Figure 2b). Also, Figure 2b and Figure 2c illustrate the increase of SCINR with the augmentation of sensors within the distributed system. Figure 2d illustrates that when INR is negligible, then the proposed detector and subspace based detector have the same detection performance and both are better than AMF detector when the CNR is high. when INR is high, then the proposed detector outperforms both the subspace detector and AMF. Note that referring to Figure 2b by increasing number of sensors the SCINR increases. However, to have a SCINR-independent comparison, Figure 2e shows that increasing the number of sensors with a fixed post processing SCINR, improves detection performance due to the RCS diversity gain, when we have fluctuant target amplitude.

5. CONCLUSION

We introduced a generic signal model suitable for a variety of distributed radar systems, including both PA and MIMO configurations. Utilizing a GLRT based detector, our detection performance analysis revealed distinct operational characteristics under different interference scenarios. Specifically, PA outperformed MIMO when the CPI time was kept constant across setups. However, when CPI time of PA was divided to number of transmit waveforms in MIMO case, and in the presence of nonhomogeneous interference, MIMO techniques generally surpassed the PA radar except in TDM configurations. In homogeneous interference situations, both system types exhibited equivalent performance.

6. REFERENCES

[1] Shunqiao Sun, Athina P. Petropulu, and H. Vincent Poor, "MIMO radar for advanced driver-assistance systems and autonomous driving: Advantages and challenges," *IEEE Signal Processing Magazine*, vol. 37, no. 4, pp. 98–117, 2020.

[2] Wei Liu, Martin Haardt, Maria S. Greco, Christoph F. Mecklenbräuker, and Peter Willett, "Twenty-five years of sensor array and multichannel signal processing: A review of progress to date and potential research directions," *IEEE Signal Processing Magazine*, vol. 40, no. 4, pp. 80–91, 2023.

[3] Stefano Fortunati, Luca Sanguinetti, Fulvio Gini, Maria Sabrina Greco, and Braham Himed, "Massive mimo radar for target detection," *IEEE Transactions on Signal Processing*, vol. 68, pp. 859–871, 2020.

[4] Jian Li and Petre Stoica, *MIMO Radar Signal Processing*, John Wiley and Sons, Inc., 2009.

[5] Minh Q. Nguyen, Reinhard Feger, Jonathan Bechter, Markus Pichler-Scheder, Martin H. Hahn, and Andreas Stelzer, "Fast-chirp fdma mimo radar system using range-division multiple-access and doppler-division multiple-access," *IEEE Transactions on Microwave Theory and Techniques*, vol. 69, no. 1, pp. 1136–1148, 2021.

[6] Mohammad Alaee-Kerahroodi, Prabhu Babu, Mojtaba Soltanalian, and MR Bhavani Shankar, *Signal Design for Modern Radar Systems*, Artech House, 2022.

[7] Sandeep Rao, "MIMO radar," Tech. Rep., Texas Instruments, 2018.

[8] Takayuki Kitamura and Kei Suwa, "Doppler division multiplexed multiple-input–multiple-output imaging using cascaded millimeter-wave radars," *IEEE Transactions on Microwave Theory and Techniques*, vol. 70, no. 3, pp. 1571–1581, 2022.

[9] Feng Xu, Sergiy A. Vorobyov, and Fawei Yang, "Transmit beamspace DDMA based automotive MIMO radar," *IEEE Transactions on Vehicular Technology*, vol. 71, no. 2, pp. 1669–1684, 2022.

[10] Eli Brookner, "MIMO radars demystified — and their conventional equivalents," in *2016 IEEE International Symposium on Phased Array Systems and Technology (PAST)*, 2016, pp. 1–10.

[11] Qian He, Nikolaus H. Lehmann, Rick S. Blum, and Alexander M. Haimovich, "Mimo radar moving target detection in homogeneous clutter," *IEEE Transactions on Aerospace and Electronic Systems*, vol. 46, no. 3, pp. 1290–1301, 2010.

[12] Shabnam Ghotbi, Moein Ahmadi, and Kamal Mohamedpour, "Moving target detection under spatially non-homogeneous clutter for airborne phased-MIMO radar," in *2015 IEEE Radar Conference*, 2015, pp. 82–86.

[13] Yao Rong, Augusto Aubry, Antonio De Maio, and Mengjiao Tang, "Adaptive radar detection in low-rank heterogeneous clutter via invariance theory," *IEEE Transactions on Signal Processing*, vol. 69, pp. 1492–1506, 2021.

[14] Wei Yi, Tao Zhou, Yue Ai, and Rick S. Blum, "Suboptimal low complexity joint multi-target detection and localization for non-coherent mimo radar with widely separated antennas," *IEEE Transactions on Signal Processing*, vol. 68, pp. 901–916, 2020.

[15] Hongbin Li, Fangzhou Wang, Cengcang Zeng, and Mark A. Govoni, "Signal detection in distributed MIMO radar with non-orthogonal waveforms and sync errors," *IEEE Transactions on Signal Processing*, vol. 69, pp. 3671–3684, 2021.

[16] Moein Ahmadi, Mohammad Alaee-Kerahroodi, Bhavani Shankar M. R., and Björn Ottersten, "Subspace-based detector for distributed mmWave MIMO radar sensors," in *ICASSP 2023 - 2023 IEEE International Conference on Acoustics, Speech and Signal Processing (ICASSP)*, 2023, pp. 1–5.

[17] Yao Rong, Augusto Aubry, Antonio De Maio, and Mengjiao Tang, "Adaptive radar detection in gaussian interference using clutter-free training data," *IEEE Transactions on Signal Processing*, vol. 70, pp. 978–993, 2022.

[18] Danilo Orlando, Giuseppe Ricci, and Louis L. Scharf, "A unified theory of adaptive subspace detection part i: Detector designs," *IEEE Transactions on Signal Processing*, vol. 70, pp. 4925–4938, 2022.

[19] F.C. Robey, D.R. Fuhrmann, E.J. Kelly, and R. Nitzberg, "A CFAR adaptive matched filter detector," *IEEE Transactions on Aerospace and Electronic Systems*, vol. 28, no. 1, pp. 208–216, 1992.